Near-Infrared Light Activated Azo-BF$_2$ Switches

Yin Yang, Russell P. Hughes, and Ivan Aprahamian*

Department of Chemistry, Dartmouth College, Hanover, New Hampshire 03755, United States
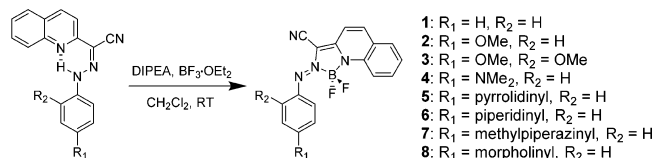
S *Supporting Information*

ABSTRACT: Increasing the electron density in BF$_2$-coodinated azo compounds through *para*-substitution leads to a bathochromic shift in their activation wavelength. When the substituent is dimethyl amine, or the like, the *trans/cis* isomerization process can be efficiently modulated using near infrared light. The electron donating capability of the substituent also controls the hydrolysis half-life of the switch in aqueous solution, which is drastically longer for the *cis* isomer, while the BF$_2$-coodination prevents reduction by glutathione.

Light penetration through tissue is primarily regulated by the absorptions of hemoglobin and water,[1] which limit its "therapeutic window" to the 600−1200 nm range. In principle, the more red-shifted the wavelength, the deeper the penetration; hence, near-infrared (NIR) is far better than red light in this aspect.[2] One way of using this property of light is to couple it with photochromic[3] compounds that are capable of reversibly modulating biological processes. This is the main objective of the fields of photopharmacology[4] and opto(chemical)genetics.[5] Azo compounds[6] are the most commonly used light activated switches[7] in these research areas because of their efficient *trans/cis* photoisomerization. However, this process generally relies on UV light, which might limit the biocompability of such switches.[8] Consequently, there has been intense activity in the field in trying to shift the activation wavelength of these photochromic compounds to the visible region[9] and beyond. The burgeoning activity has led to the development of a number of visible light-activated azo compounds, through appropriate derivatization,[10] or the use of metal to ligand charge transfer,[11] among other approaches.[12] This activity has recently paid off with the seminal work by Woolley et al. describing the in vivo activation of an azo compound using red light (635 nm).[10c] Despite these recent advances there is still a need to develop more efficient systems and push the activation wavelength of the azo compounds beyond the red region, in order to gain access to deeper tissues.[13] In this context, Qian et al. have recently showed[14] how NIR activated upconversion nanoparticles[15] can be used in manipulating azo compounds; however, this was accomplished using the NIR light indirectly, as the azo switch was still modulated using the UV light emitting from the excited nanoparticles. Furthermore, the incorporation of nanoparticles complicates the system and leads to low isomerization efficiencies, reducing the practicality of this approach in photopharmacology and opto(chemical)genetics.

We have recently discovered[16] that the coordination of BF$_2$ with an azo group's nitrogen lone-pair leads to a reversal of the positions of *n-π** and *π−π** transition energy levels. This property enabled us to switch the azo-compounds using visible (i.e., blue and green) light. Density functional theory (DFT) calculations predicted that increasing the electron-density in the system could further red-shift the absorption bands and hence activation wavelength of the system. To test this hypothesis, we designed a series of azo-BF$_2$ complexes having electron donating *para*- and *ortho*-substituents (Scheme 1).[17] Here we report how

Scheme 1. Synthesis of *Ortho*- and *Para*-substituted BF$_2$-Coordinated Azo Complexes

1: R$_1$ = H, R$_2$ = H
2: R$_1$ = OMe, R$_2$ = H
3: R$_1$ = OMe, R$_2$ = OMe
4: R$_1$ = NMe$_2$, R$_2$ = H
5: R$_1$ = pyrrolidinyl, R$_2$ = H
6: R$_1$ = piperidinyl, R$_2$ = H
7: R$_1$ = methylpiperazinyl, R$_2$ = H
8: R$_1$ = morpholinyl, R$_2$ = H

such substituents shift the azo-BF$_2$ absorption bands to the red and even NIR region, thus enabling us (for the first time to the best of our knowledge) to directly and efficiently activate the isomerization of an azo-compound using NIR light.[18] We also show how these systems are stable to glutathione reduction and have relatively long-lived half-lives in aqueous solutions.

As predicted by DFT calculations, the introduction of a methoxy group *para* to the azo linkage (Scheme 2) leads to a

Scheme 2. Visible Light-Induced *Trans/Cis* Isomerization of 2
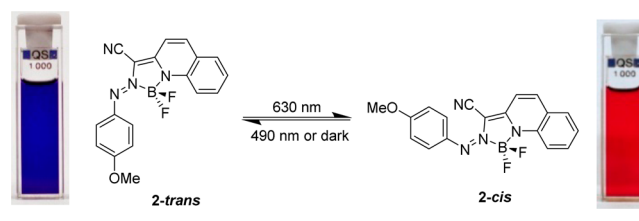
bathochromic shift in the *π−π** band of **2** (λ_{max} = 594 nm; ε = 15,998 M^{-1} cm^{-1}). The λ_{max} of the *cis* photostationary state (PSS; irradiation at 630 nm) of compound **2** is red-shifted by 40 nm (Figure 1a), while the *trans* PSS (irradiation at 490 nm) is red-shifted by 55 nm compared with the parent complex **1**.[16] The switching process of **2** was accompanied by a strong color change between cobalt blue and poppy red. High photoconversion ratios (PSS490 = 92% *trans*; PSS630 = 96% *cis*) and a 93% *trans* isomer ratio under dark were determined for **2** using ^{1}H NMR spectroscopic analysis (Figures S4 and S3 in the Supporting Information). There are several spectral features of **2** that set it
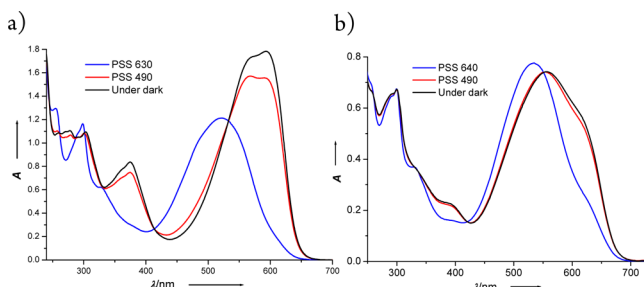
a)

b)

Figure 1. (a) UV/vis spectral changes upon the photoisomerization of **2** in CH$_2$Cl$_2$ (0.2 mM). The black trace is of **2** equilibrated under dark (mainly *trans*), which upon irradiation at λ = 630 nm gives the *cis* PSS (blue trace). Irradiating the latter at λ = 490 nm gives the *trans* PSS (red trace). (b) UV/vis spectral changes upon the photoisomerization of **3** in CH$_2$Cl$_2$ (0.1 mM). The black trace is of **3** equilibrated under dark, which upon irradiation at λ = 640 nm gives the *cis* PSS (blue trace). Irradiating the latter at λ = 490 nm gives the *trans* PSS (red trace).

apart from the parent compound; instead of a sharp band, the $\pi-\pi^*$ band of the *trans*-dominant state exhibits a well-resolved vibrational fine structure, with the highest-intensity peak observed at λ_{max} = 594 nm. The appearance of the sub-bands can be attributed to the intensified vibrational transitions caused by the electron-donating *para*-substituent.[19] In addition, the isomerization process in **2** is more efficient than **1** based on its quantum yields ($\Phi_{trans \rightarrow cis}$ = 71% and $\Phi_{cis \rightarrow trans}$ = 95%). This efficiency enhancement results from a better separation of the *cis* and *trans* states' $\pi-\pi^*$ bands, which leads to less overlap of their irradiation windows compared to the parent azo complex **1**. The *cis* isomer of **2** has a half-life of 10.4 h at 294 K in deoxygenated methylene chloride (Figure S25 in the Supporting Information), compared to 25 min in regular solvent (not deoxygenated).[16,20]

Hecht et al. recently identified[10b] that *ortho*-tetrafluoroazo-benzene has a slightly blue-shifted $\pi-\pi^*$ absorption when compared to its parent azobenzene. In 2011, Woolley's group reported[10a] that the substitution of the *ortho* positions with methoxy groups leads to the separation of the $n-\pi^*$ orbital of the *cis* and *trans* isomers and a red-shift of the $\pi-\pi^*$ band in the latter. In order to study the *ortho*-substitution effect on our system, we prepared complex **3** (Scheme 3). The extra *ortho*-

Scheme 3. Visible Light-Induced *Trans/Cis* Isomerization of 3
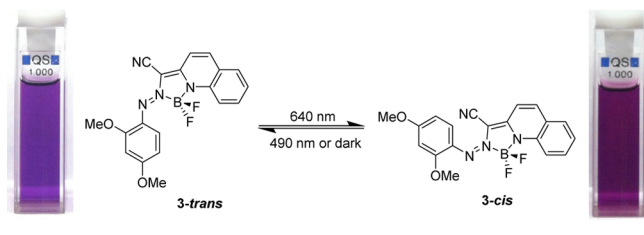
methoxy group in **3** causes a 20 nm blue shift of its *trans* absorption band relative to **2** (Figure 1b), whereas its *cis* isomer's $\pi-\pi^*$ band is red-shifted by 15 nm. The combined effect is the generation of a pronounced overlap between the absorption bands of the two configurations. This overlap resulted in a drastic decrease in the efficiency of the switch, including its PSS ratios (PSS490 = 56% and PSS640 = 79%) and photoswitching quantum yields ($\Phi_{cis \rightarrow trans}$ = 51% and $\Phi_{trans \rightarrow cis}$ = 42%). We hypothesize that the steric hindrance of the *ortho*-OMe group destabilizes the *trans* isomer and prevents the phenyl ring from lying coplanar with the rest of the molecule. The loss of planarity

in the *trans* isomer can be inferred by its blue-shifted absorption band, and its destabilization is evident from the lower *trans* isomer ratio (58%) under dark.

Encouraged by the results from compound **2**, we shifted our focus to the BF$_2$-azo complexes **4−8**, which were synthesized with the intention of further pushing the activation wavelength of the systems to even lower energy levels. The attachment of a *para*-dimethylamino group shifted the absorption peak of complex **4** to 680 nm (ε = 36 255 M^{-1} cm^{-1}) with a tail extending out to 760 nm (Figure 2). This property allowed us to
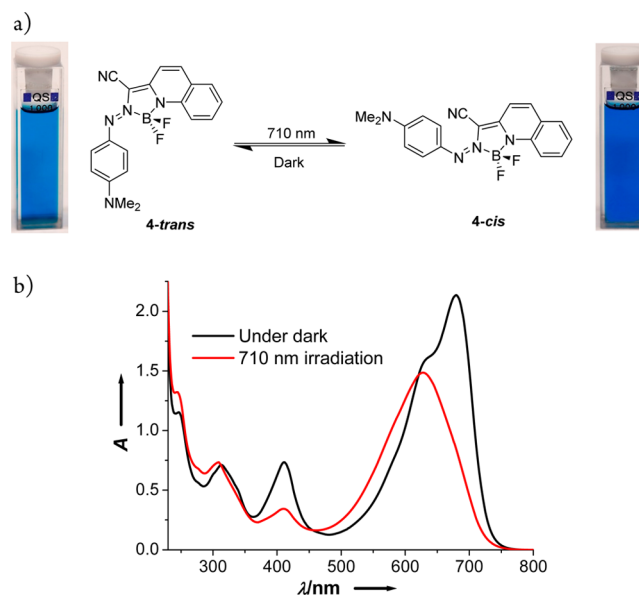
a)

b)

Figure 2. (a) NIR light-induced *trans/cis* isomerization of **4**. (b) UV/vis spectral changes upon the photoisomerization of **4** in CH$_2$Cl$_2$ (0.2 mM). The black trace is of **4** equilibrated under dark (mainly *trans*), which upon irradiation at λ = 710 nm gives the *cis* populated state (red trace).

activate the *trans* to *cis* isomerization process using NIR light! The UV/vis spectrum of the *trans* isomer of **4** exhibits better-resolved vibrational fine structure compared to **2**. The half-life of the *cis* isomer of **4** was determined to be 250 s (Figure S26 in the Supporting Information), with no obvious difference in rate observed by deoxygenating the methylene chloride solution. Such an enhancement in the thermal relaxation rate compared to the parent compound **1** ($t_{1/2}$ = 12.5 h)[16] is not surprising. The effective bond order of N=N bond is strongly influenced by the substituents on the phenyl rings (vide infra). Electron-donating groups would cause an increase in the electron density of the π^* (antibonding) orbital and thus a decrease in the effective bond order of the N=N bond, which leads to a lower thermal isomerization barrier.[6,21] Under dark, complex **4** is almost quantitatively (97%) composed of the thermodynamically more stable *trans* form. Upon irradiation with 710 nm light, isomerization to the *cis* isomer occurs quickly. Because of the fast *cis* to *trans* isomerization rate, we were unable to record the PSS at 710 nm. The lowest estimation of the amount of *cis* isomer at PSS710 is 63% based on ^{1}H NMR spectroscopy (Figure S12 in the Supporting Information).[22]

Next we studied the isomerization and photochromic properties of the pyrrolidinyl (**5**), piperidinyl (**6**), methylpiper-izinyl (**7**), and morpholinyl (**8**) BF$_2$-azo derivatives (Figure 3, and Figure S31 in Supporting Information). As can be seen by their UV/vis spectra, switches **5** and **6−8** undergo isomerization
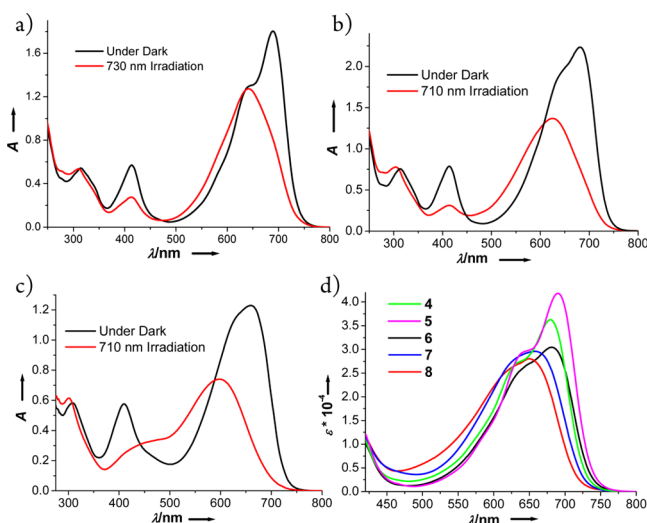
Figure 3. UV/vis spectral changes upon photoisomerization of (a) **5**, (b) **6**, and (c) **7**. The black trace is the equilibrated complex in the dark (mainly *trans*), which upon irradiation at λ = 710 or 730 nm gives the *cis* populated state (red trace). (d) Overlay of the $\pi-\pi^*$ absorption bands of the *trans* isomers of **4−8**, represented by green, magenta, black, blue, and red lines, respectively.

Figure 4. (a) Switching cycles of **4** in acetonitrile/PBS buffer (1:1) monitored by following the absorbance at λ = 681 nm (black trace) upon irradiation at λ = 710 nm then leaving in the dark. (b) UV/vis spectra following an acetonitrile/PBS buffer (1:1) solution of the azo-BF$_2$ complex **4** at 25 °C. The interval between each scan is 20 min.

upon irradiation with 730 and 710 nm light, respectively, and maintain a high ratio of *trans* isomer under dark (98%, 98%, 97% and 94% *trans* ratio, with molar extinction coefficient ε = 41 839, 30 458, 29 536, and 28 025 M^{-1} cm^{-1}, for **5**, **6**, **7**, and **8**, respectively). The small variation in the electronic characteristics of the amino groups greatly impacts their photophysical properties, including their absorption bands and half-lives. The overlay of the absorption bands of compounds **4−8** (Figure 3d) reveals that the resolution of their vibrational fine structure decreases in the order of **5** > **4** > **6** > **7** > **8**, which is in accordance to their *para*-substituent's electron-donating ability.[23] A similar trend is also observed in their absorption maxima (λ_{max} = 690, 681, 661, and 652 nm for **5**, **6**, **7**, and **8**, respectively). In addition, the half-life relaxation rate from *cis* to *trans* is substantially enhanced in switch **8** ($t_{1/2}$ = 900 s) as compared to **5** ($t_{1/2}$ = 120 s), **6** ($t_{1/2}$ = 150 s), and **7** ($t_{1/2}$ = 400 s), which is again in accordance with their electron donation capability. Such a dramatic change in the half-life of these switches was also reflected by their PSS values. The highest PSS ratio for **5** that we could measure was 23%, while for **6**, **7**, and **8** it was 28%, 49%, and 83%, respectively. The latter value is comparable to that obtained for the parent azo-BF$_2$ complex **1**.

To test the stability of the switches in an aqueous environment, we conducted multiple switching cycles (10 cycles shown in Figure 4a) of **4** in an acetonitrile/PBS buffer (1:1) mixed solvent system. These experiments were conducted by irradiating the sample using 710 nm light, followed by thermal relaxation under dark. Although switch **4** is stable for short periods of time under these conditions, it gradually undergoes hydrolysis (Figure S32 in the Supporting Information), reverting back to the starting hydrazone[24] compound (Figure 4b) with a half-life of 2.3 h. We also tested the stability of switch **4** to reduction by glutathione (GSH). The switch was incubated in 10 mM reduced glutathione in acetonitrile/PBS buffer (1:1) solution. No obvious difference was observed in its degradation half-life ($t_{1/2}$ = 2.5 h)[25] compared to that measured in the acetonitrile/PBS buffer (Figure S33 in the Supporting Information). The multiple isosbestic points observed in both cases (λ = 286, 413, and 537 nm) suggest the
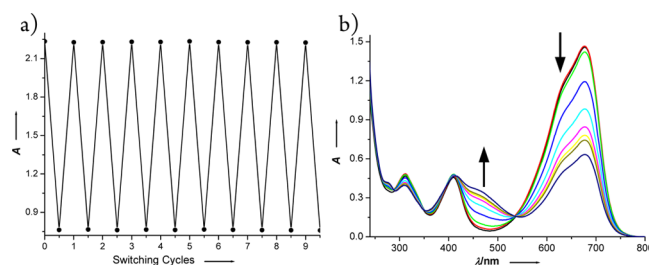
existence of only two species in solution, which in this case are the azo-BF$_2$ complex and the hydrazone starting material. These results, along with similar stability tests conducted for compounds **5−8** (Figures S34−S41 in the Supporting Information), demonstrate the robustness of this class of NIR switches in high concentrations of GSH. Moreover, they indicate that coordination with BF$_2$ might be a viable strategy to preventing glutathione reduction of azo compounds.

By comparing the degradation half-life of the complexes in PBS buffer (2.6, 2.3, 2.0, 1.2, and 0.9 h for **5**, **4**, **6**, **7**, and **8**, respectively), we can conclude that the higher electron-donating ability of the *para*-substituent, the more stable the switch is to hydrolysis. According to the crystallographic analysis (Figure 5),
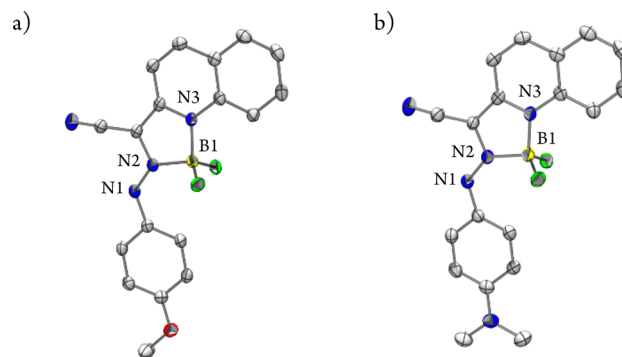

Figure 5. ORTEP drawing (50% probability ellipsoids) of the crystal structures of (a) **2** and (b) **4**. The hydrogen atoms were removed for clarity.

the stronger the electron-donating capability of the *para*-substituent, the longer the N(1)=N(2) bond (1.294(1) and 1.298(2) Å in **2** and **4**, respectively) and shorter the B(1)−N(3) bond and B(1)−N(2) bond lengths become (1.550(2) and 1.624(2) Å in **2**, and 1.542(2) and 1.615(2) Å in **4**, respectively). We speculate that the latter trend (i.e., the strengthening of the BN bonds) makes the compounds less susceptible to hydrolysis.

Remarkably, we found out that switch **4** is relatively stable toward hydrolysis if it is kept in its *cis* form through constant irradiation with 710 nm light. We monitored aqueous solutions of **4** (with and without glutathione) using UV/vis spectroscopy (Figure 6) and observed at most 6% hydrolysis over a period of 8 h. To have a better understanding of this phenomenon we calculated the *cis* and *trans* isomers of **4** (Figure S47 and S48 in the Supporting Information) and found out that the B(1)−N(2) bond (Figure 5) in the *cis* isomer is shorter by 0.02 Å compared to the *trans* form. The same trend was found for compounds **1**, **5**,
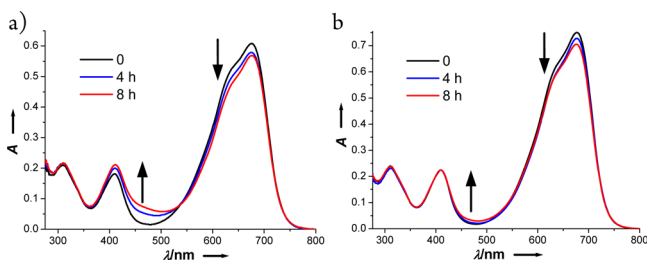
Figure 6. UV/vis spectra following (a) an acetonitrile/PBS buffer (1:1) solution and (b) an acetonitrile/PBS buffer (1:1) with 10 mM reduced glutathione solution of the azo-BF$_2$ complex **4** kept under continuous irradiation with 710 nm light at 25 °C. The interval between each scan is 4 h.

and **6** (Figures S46−S52 in the Supporting Information) indicating that this is a general trend. This finding corroborates our speculation that strengthening the BN bonds (in this case the B(1)−N(2) bond, which happens to be the longest/weakest of the two bonds) contributes to the stability of the system toward hydrolysis.

In conclusion, we have shown how the *para*-substitution of azo-BF$_2$ compounds with electron donating groups leads to photochromic compounds that can be activated with NIR light. Structure−property analysis showed that the hydrolysis process in these systems can be modulated and slowed down using strong electron donating *para*-substituents. Moreover, we showed that the *cis* isomer is drastically more stable toward hydrolysis than the *trans* isomer and that these switches are not susceptible to reduction by glutathione, most probably because of the coordination with BF$_2$. These results are very promising and pave the way for using these BF$_2$-coordinated azo compounds in photopharmacolgical[4] and opto(chemo)genetical[5] applications.

■ ASSOCIATED CONTENT

ⓢ Supporting Information

Experimental procedures, NMR spectra of key compounds, photoisomerization studies, kinetic measurements, X-ray crystallography, and computational data. This material is available free of charge via the Internet at http://pubs.acs.org.

■ AUTHOR INFORMATION

Corresponding Author

ivan.aprahamian@dartmouth.edu

Notes

The authors declare no competing financial interest.

■ ACKNOWLEDGMENTS

■ REFERENCES

(1) Kalka, K.; Merk, H.; Mukhtar, H. *J. Am. Acad. Dermatol.* **2000**, *42*, 389−413.

(2) Smith, K. C., Ed. *The Science of Photobiology*; Plenum Press: New York, 1977.

(3) (a) Irie, M. *Chem. Rev.* **2000**, *100*, 1683−1684. (b) Durr, H.; Bouas-Laurent, H., Eds. *Photochromism: Molecules and Systems*; Elsevier: Amsterdam, The Netherlands, 2003.

(4) Velema, W. A.; Szymanski, W.; Feringa, B. L. *J. Am. Chem. Soc.* **2014**, *136*, 2178−2191.

(5) Sjulson, L.; Miesenbçck, G. *Chem. Rev.* **2008**, *108*, 1588−1602. (b) Fehrentz, T.; Schönberger, M.; Trauner, D. *Angew. Chem., Int. Ed.* **2011**, *50*, 12156−12182. (b) Brieke, C.; Rohrbach, F.; Gottschalk, A.; Mayer, G.; Heckel, A. *Angew. Chem., Int. Ed.* **2012**, *51*, 8446−8476.

(6) Bandara, H. M. D.; Burdette, S. C. *Chem. Soc. Rev.* **2012**, *41*, 1809−1825.

(7) (a) Kay, E. R.; Leigh, D. A.; Zerbetto, F. *Angew. Chem., Int. Ed.* **2007**, *46*, 72−191. (b) Balzani, V.; Credi, A.; Venturi, M. *Molecular Devices and Machines: Concepts and Perspectives for the Nanoworld*; Wiley-VCH: Weinheim, Germany, 2008. (b) Stoddart, J. F. *Chem. Soc. Rev.* **2009**, *38*, 1802−1820. (d) Feringa, B. L.; Browne, W. R., Eds. *Molecular Switches*; Wiley-VCH: Weinheim, Germany, 2011.

(8) (a) Brash, D.; Rudolph, J.; Simon, J.; Lin, A.; Mckenna, G.; Baden, H.; Halperin, A.; Ponten, J. *Proc. Natl. Acad. Sci. U.S.A.* **1991**, *88*, 1012−10128. (b) Tamai, T. K.; Vardhanabhuti, V.; Foulkes, N. S.; Whitmore, D. *Curr. Biol.* **2004**, *14*, R104−R105. (c) Banerjee, G.; Gupta, N.; Kapoor, A.; Raman, G. *Cancer Lett.* **2005**, *223*, 275−284.

(9) (a) Sadovski, O.; Beharry, A. A.; Zhang, F.; Woolley, G. A. *Angew. Chem., Int. Ed.* **2009**, *48*, 1484−1486. (b) Wegner, H. A. *Angew. Chem., Int. Ed.* **2012**, *51*, 4787−4788.

(10) (a) Beharry, A. A.; Sadovski, O.; Woolley, G. A. *J. Am. Chem. Soc.* **2011**, *133*, 19684−19687. (b) Bleger, D.; Schwarz, J.; Brouwer, A.; Hecht, S. *J. Am. Chem. Soc.* **2012**, *134*, 20597−20600. (c) Samanta, S.; Beharry, A. A.; Sadovski, O.; McCormick, T. M.; Babalhavaeji, A.; Tropepe, V.; Woolley, G. A. *J. Am. Chem. Soc.* **2013**, *135*, 9777−9784. (d) Samanta, S.; McCormick, T. M.; Schmidt, S. K.; Seferos, D. S.; Woolley, G. A. *Chem. Commun.* **2013**, *49*, 10314−10316.

(11) (a) Kurihara, M.; Hirooka, A.; Kume, S.; Sugimoto, M.; Nishihara, H. *J. Am. Chem. Soc.* **2002**, *124*, 8800−8801. (b) Venkataramani, S.; Jana, U.; Dammaschk, M.; Sönnichsen, F. D.; Tuczek, F.; Herges, R. *Science* **2011**, *331*, 445−448.

(12) Siewertsen, R.; Neumann, H.; Buchheim-Stehn, B.; Herges, R.; Nather, C.; Renth, F.; Temps, F. *J. Am. Chem. Soc.* **2009**, *131*, 15594−15595.

(13) Light at 630 nm penetrates only the first 5 mm of tissue, while light between 700 and 800 nm has a penetration of 1−2 cm. See ref 2.

(14) Wang, L.; Dong, H.; Li, Y.; Xue, C.; Sun, L.-D.; Yan, C.-H.; Li, Q. *J. Am. Chem. Soc.* **2014**, *136*, 4480−4483.

(15) Sun, L.-D.; Wang, Y.-F.; Yan, C.-H. *Acc. Chem. Res.* **2014**, *47*, 1001−1009.

(16) Yang, Y.; Hughes, R. P.; Aprahamian, I. *J. Am. Chem. Soc.* **2012**, *134*, 15221−15224.

(17) The *para*- and/or *ortho*-substituted derivatives were synthesized following the synthetic protocol used in the making of the parent complex **1**. See ref 16.

(18) For a NIR absorbing BF$_2$-azo compound that does not switch, please see: Li, Y.; Patrick, B. O.; Dolphin, D. *J. Org. Chem.* **2009**, *74*, 5237−5243.

(19) Mustroph, H. *Dyes Pigm.* **1991**, *15*, 129−137.

(20) The nature of the effect of oxygen on the isomerization rate is under investigation.

(21) Blevins, A. A.; Blanchard, G. J. *J. Phys. Chem. B* **2004**, *108*, 4962−4968.

(22) We are unable to measure the quantum yield of the process because of the competition with the fast thermal isomerization process and instrumentation limitations.

(23) Mustroph, H. *Dyes Pigm.* **1991**, *16*, 223−230.

(24) (a) Ray, D.; Foy, J. T.; Hughes, R. P.; Aprahamian, I. *Nat. Chem.* **2012**, *4*, 757−762. (b) Su, X.; Voskian, S.; Hughes, R. P.; Aprahamian, I. *Angew. Chem., Int. Ed.* **2013**, *52*, 10734−10739. (c) Tatum, L.; Su, X.; Aprahamian, I. *Acc. Chem. Res.* **2014**, *47*, 2141−2149. (d) Su, X.; Aprahamian, I. *Chem. Soc. Rev.* **2014**, *43*, 1963−1981.

(25) The hydrolysis half-life in the glutathione containing solutions is in general slightly longer than in the regular acetonitrile/PBS buffer (1:1) mixtures. We currently have no hypothesis to explain this effect.

13193

dx.doi.org/10.1021/ja508125n | *J. Am. Chem. Soc.* 2014, 136, 13190−13193